ISSN 2070-2051, Protection of Metals and Physical Chemistry of Surfaces, 2015, Vol. 51, No. 5, pp. 899–907. © Pleiades Publishing, Ltd., 2015.

PHYSICOCHEMICAL PROBLEMS OF MATERIALS PROTECTION

Electrochemical Investigations on the Inhibition Behavior and Adsorption Isotherm of Synthesized di-(Resacetophenone)-1,2-cyclohexandiimine Schiff base on the Corrosion of Steel in 1 M HCl[1]

A. Karimi[a], I. Danaee[a], H. Eskandari[a], and M. RashvanAvei[b]

[a] *Abadan Faculty of Petroleum Engineering, Petroleum University of Technology, Abadan, Iran*

e-mail: danaee@put.ac.ir

[b] *Department of Chemistry, K. N. Toosi University of Technology, Tehran, Iran*

Received February 04, 2015

Abstract—The potential of di-(Resacetophenone)-1,2-cyclohexandiimine as an environmentally friendly corrosion inhibitor for steel has been investigated in 1 M HCl using potentiodynamic polarization, electrochemical impedance spectroscopy and chronoamperometry measurements. All electrochemical measurements suggest that this compound is an excellent corrosion inhibitor for mild steel and the inhibition efficiency increases with the increase in inhibitor concentration. The effect of temperature on the corrosion behavior of mild steel with the addition of the Schiff base was studied in the temperature range from 25 to 65°C. Adsorption of this inhibitor follows the Langmuir adsorption isotherms. The value of Activation energy and the thermodynamic parameters such as ΔH_{ads}, ΔS_{ads}, ΔK_{ads} and ΔG_{ads} were calculated by the corrosion currents at different temperatures and using the adsorption isotherm. The morphology of mild steel surface in the absence and presence of inhibitor was examined by scanning electron microscopy (SEM) images.

DOI: 10.1134/S2070205115050147

1. INTRODUCTION

Corrosion is a fundamental process playing an important role in economics and safety, particularly for metals and alloys. Steel has found wide application in a broad spectrum of industries and machinery [1, 2]. In most industrial processes, acidic solution are commonly used for the pickling, industrial acid cleaning, acid descaling, oil well acidifying, etc. Unfortunately, iron and its alloys could corrode during these acidic applications particularly with the use of hydrochloric acid and sulphuric acid, which results in terrible waste of both resources and money [3, 4].

Corrosion prevention systems favor the use of corrosion inhibitors with low or zero environmental impacts. Inhibitors are chemicals that react with a metallic surface or the environment. Inhibitors decrease corrosion processes by increasing the anodic or cathodic polarization behavior, decreasing the movement or diffusion of ions to the metallic surface and increasing the electrical resistance of the metallic surface [5, 6].

The inhibiting actions of organic compounds are usually attributed to their interactions with the metal surface via their adsorption. These compounds in general are adsorbed on the metal surface, blocking the active corrosion sites. Three types of adsorption may take place by organic molecules at metal/solution interface: (a) electrostatic attraction between the charged molecules and the charged metal, (b) interaction of unshared electron pairs or π electron in the molecule with the metal, and (c) combination of (a) and (b) [7, 8].

The choice of the inhibitor is based on two considerations, first economic consideration and second, should contain the electron cloud on the aromatic ring or the electronegative atoms such as N, O in the relatively long chain compounds. Generally the organic compounds containing hetero atoms like O, N, S, and P are found to work as very effective corrosion inhibitors. The efficiency of these compounds depends upon electron density present around the hetero atoms, the number of adsorption active centers in the molecule and their charge density, molecular size, mode of adsorption, and formation of metallic complexes [9, 10]. These features obviously can be combined within the same molecule such as Schiff bases. In the past few years, the inhibition of various metals such as iron, copper, zinc, aluminum, and carbon steel corrosion in acid solutions by Schiff bases with environmental considerations has attracted more attention [12, 13]. Schiff bases can conveniently be synthesized from relatively cheap starting materials. It is also reported that Schiff bases show more inhibition efficiency than corresponding amines [14].

The goal of this work is to investigate the effect of synthesized Schiff base corrosion inhibitor di-(Resacetophenone)-1,2-cyclohexandiimine (R-DACH) on

[1] The article is published in the original.

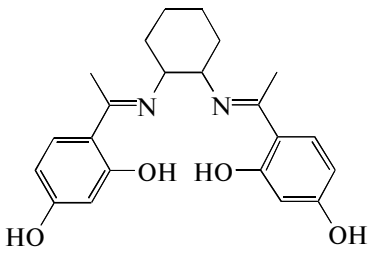

Fig. 1. The general structure of investigated Schiff bases.

the corrosion of mild steel in 1 M HCl, evaluated by Tafel polarization and electrochemical impedance spectroscopy (EIS) data. Effects of concentration and temperature on the inhibition efficiencies of the selected Schiff base have been studied systematically. Thermodynamic parameters such as enthalpy, entropy and Gibbs free energy were calculated from experimental data of the inhibition process at different temperature.

2. MATERIALS AND METHODS

2.1. Preparation of di-(Resacetophenone)-1,2-cyclohexandiimine (R-DACH)

All chemicals used in present work were of reagent-grade Merck product and used as received without further purification. The R-DACH Schiff base (Fig. 1) was prepared in high yeild (94%) by the condensation of Resacetophenone (0.304 g, 2 mmol) with Cyclohexanediamine (0.114 g, 1 mmol) in a stirred ethanolic solution and heated to reflux for 5 h according to the described procedure [6]. The resulting dirty yellow color precipitate was filtered off, washed with warm ethanol and diethyl ether. Identification of structure of synthesized Schiff base was performed by IR and ^{1}HNMR spectroscopy and elemental analysis.

2.2. Sample Preparation

Working electrodes were prepared from steel X52 specimens of the chemical composition: C 0.3, Mn 1.350, P 0.03, S 0.03 wt.%, and the balance Fe. Samples were cut from a flat plate by the wire cut method. The dimension of each sample is 1 cm × 1 cm. Working electrodes were prepared by embedding the sample in epoxy resin, exposing a geometrical surface area of 1 cm^2 to the aggressive electrolyte. The exposed areas of the electrodes were mechanically abraded with 400, 800, 1200 and 2000 grades of emery paper, rinsed by distilled water and degreased with acetone before each electrochemical experiment.

The measurements were performed in 1 M HCl in the absence and presence of Schiff bases in the concentration range from 5×10^{-5} to 2×10^{-3} M. Chemicals used in corrosion experiments were from Merck grade and used without further purification. Distilled water was used to prepare test solutions.

2.4. Electrochemical Measurements

Electrochemical measurements were carried out in a conventional three-electrode system. A reference electrode was a saturated calomel electrode (SCE) and the auxiliary electrode was a platinum sheet. All experiments were repeated three times. To reach the steady state condition, before each experiment, the working electrode was immersed in the test cell for 20 min. The electrochemical measurements were carried out using computer controlled ZAHNER potentiostat/galvanostat. Electrochemical impedance spectroscopy (EIS) was recorded in frequency range of 100 kHz to 10 mHz with 0.01 V peak-to-peak amplitude using AC signals at open circuit potential. Polarization curves were scanned at a scan rate of 1 mV s^{-1} from −700 to −100 mV. All tests were done at constant temperature by controlling the cell temperature using a water bath. Polarization curve was used to calculate corrosion current density by the Tafel extrapolation method. The polarization resistance was calculated from the slope of the potential versus logarithm of current plots. Fitting of experimental impedance spectroscopy data to the proposed equivalent circuit was done by means of home written least square software based on the Marquardt method for the optimization of functions and Macdonald weighting for the real and imaginary parts of the impedance [15, 16].

The morphology of steel surface after 12 h exposure to 1 M HCl solution in the absence and presence of 2×10^{-3} M R-DACH was observed by scanning electron microscope (SEM) model VEGA.

3. RESULTS AND DISCUSSION

3.1. Tafel Polarization Measurements

Figure 2 shows the anodic and cathodic polarization plots of steel in 1 M HCl in the absence and presence of different concentrations of inhibitor at 25°C. Table 1 gives the electrochemical corrosion parameters such as corrosion potential (E_{corr} vs. SCE), corrosion current density (J_{corr}), cathodic and anodic Tafel slopes (β_a, β_b), the degree of surface coverage (θ) and inhibition efficiency (*IE*) obtained by extrapolation of the Tafel lines. The degree of surface coverage and inhibition efficiency are calculated using the following equations [17]:

$$\theta = \frac{\dot{J}_{corr} - J_{corr}}{\dot{J}_{corr}}, \quad (1)$$

$$IE\% = \theta \times 100, \quad (2)$$

where *IE* is the inhibition efficiency, J_{corr} and $\dot{J}_{corr}$ are the corrosion current densities determined by the intersection of the extrapolated Tafel lines and the corrosion potential for mild steel in uninhibited and

inhibited acid solution, respectively. Both the anodic and cathodic reactions of mild steel corrosion inhibited in presence of the inhibitor. This result suggests that the addition of the R-DACH decreases the anodic dissolution and also retards the hydrogen evolution reaction. However, the influence was more pronounced in the anodic polarization plots compared to that of the cathodic polarization plots. The corrosion potential displayed small change and the curves changed slightly towards the negative direction. These results indicated that the presence of R-DACH compound inhibited iron oxidation and the hydrogen and oxygen evolution. Consequently these compounds can be classified as the mixed corrosion inhibitors, as electrode potential displacement is lower than 85 mV in any direction [18].

It can be seen that and inhibition efficiency (*IE*) increased by increasing inhibitor concentration which indicates that more inhibitor molecule are absorbed on the metal surface thus providing wider surface coverage and these compound are acting as adsorption inhibitor.

Polarization resistance (R_p) values were determined using Stern-Geary equation which is given below [19]:

$$R_p = \frac{b_a b_c}{2.303(b_a + b_c)}\left(\frac{1}{I_{\text{corr}}}\right). \quad (3)$$

By increasing the R-DACH concentration, the polarization resistance increases in the presence of compound, indicating adsorption of the inhibitor on the metal surface to block the active sites efficiently and inhibit corrosion [20].

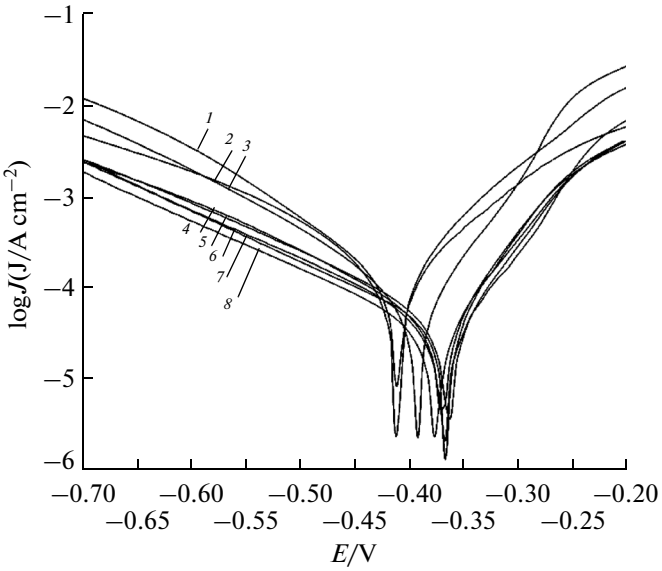

Fig. 2. Anodic and cathodic polarization curves of steel electrode in 1 M HCl without and with various concentration of inhibitor at 25°C: (1) Blank, (2) 5×10^{-5}, (3) 1×10^{-4}, (4) 2×10^{-4}, (5) 3×10^{-4}, (6) 5×10^{-4}, (7) 1×10^{-3}, (8) 2×10^{-3}M.

3.2. Electrochemical Impedance Spectroscopy

Figure 2 shows Nyquist plots recorded for the corrosion of steel in 1 M HCl solution without and with different concentrations of inhibitor obtained at E_{corr}. The plots show a depressed capacitive loop which arises from the time constant of the electrical double layer and charge transfer resistance. The impedance of the inhibited steel increases with increasing the R-DACH concentrations and consequently the inhibition efficiency increases. The equivalent circuit compatible with the Nyquist diagram recorded in the presence of inhibitor is depicted in Fig. 4. The simplest approach requires the theoretical transfer function $Z(\omega)$ to be represented by a parallel combination of a resistance R_{ct} and a capacitance C_{dl}, both in series with another resistance R_s [21]:

$$Z(\omega) = R_s + \frac{1}{i\omega C_{\text{dl}} + \frac{1}{R_{\text{ct}}}}, \quad (4)$$

where o is the frequency in rad/s, $\omega = 2\pi f$ and f is frequency in Hz. To obtain a satisfactory impedance simulation of steel, it is necessary to replace the capacitor (C) with a constant phase element (CPE) Q in the equivalent circuit [22]. The most widely accepted explanation for the presence of CPE behavior and

Table 1. Potentiodynamic polarization parameters for the corrosion of steel in 1 M HCl solution in the absence and presence of different concentrations of inhibitor at 25°C

Concentration, M	β_c, mV	β_a, mV	J_{corr}, μA cm^{-2}	$-E$, mV	R_p, Ω cm^{-2}	θ	*IE*
Blank	161	88	231.00	406.90	106.96	–	–
5×10^{-5}	150	83	115.00	400.00	201.75	0.50	50.22
1×10^{-4}	158	86	84.00	373.00	287.87	0.64	63.64
2×10^{-4}	155	85	62.00	371.00	384.75	0.73	73.16
3×10^{-4}	153	84	51.30	381.00	458.29	0.78	77.79
5×10^{-4}	149	68	38.00	370.40	533.53	0.84	83.55
1×10^{-3}	153	67	33.60	357.50	600.91	0.85	85.45
2×10^{-3}	126	61	24.60	364.40	723.08	0.89	89.35

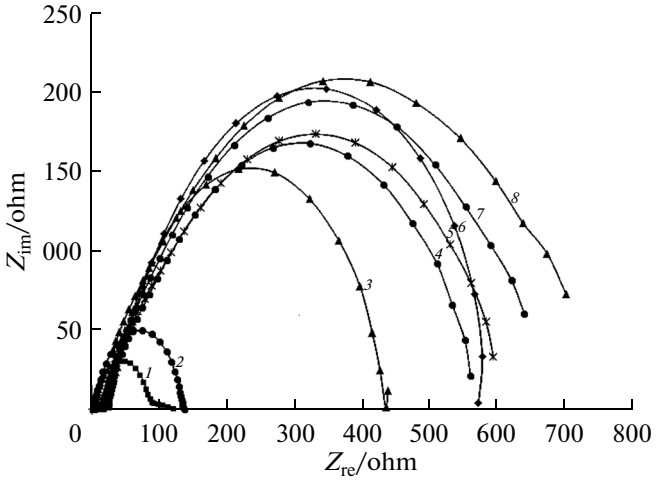

Fig. 3. Nyquist plots for steel in 1 M HCl without and with various concentration of inhibitor at 25°C: (1) Blank, (2) 5×10^{-5}, (3) 1×10^{-4},(4) 2×10^{-4}, (5) 3×10^{-4}, (6) 5×10^{-4}, (7) 1×10^{-3}, (8) 2×10^{-3} M.

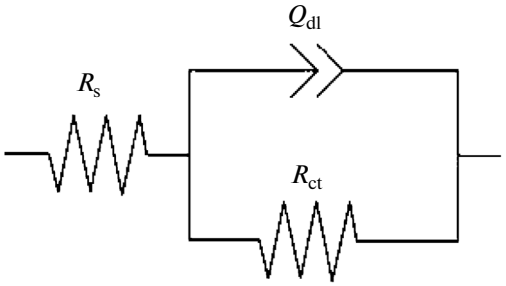

Fig. 4. Equivalent circuits compatible with the experimental impedance data for corrosion of steel electrode in different inhibitors concentrations.

depressed semicircles on solid electrodes is microscopic roughness, causing an inhomogeneous distribution in the solution resistance as well as in the double layer capacitance [22]. Constant phase element Q_{dl}, R_s and R_{ct} can be corresponded to double layer capacitance, $Q_{dl} = R^{n-1}C_{dl}^{n}$ solution resistance and charge transfer resistance, respectively. To corroborate the equivalent circuit, the experimental data are fitted to equivalent circuit and the circuit elements are obtained. Table 2 illustrates the equivalent circuit parameters for the impedance spectra of corrosion of steel in 1 M HCl solution. The results demonstrate that the presence of inhibitor enhanced the value of R_{ct} obtained in the pure medium while the values of Q_{dl} decreased. The decrease in Q_{dl} is caused by adsorption of inhibitor, indicating that the exposed area decreases. On the other hand, a decrease in Q_{dl}, which can result from a decrease in local dielectric constant and/or an increase in the thickness of the electrical double layer, suggests that Schiff base inhibitor acts by adsorption at the metal/solution interface [23].

The increase in values of R_{ct} and the decrease in values of Q_{dl} with increasing the concentration also indicate that Schiff base acts as primary interface inhibitor and the charge transfer controls the corrosion of steel under the open circuit conditions.

3.3. Effect of Temperature

The adsorption phenomenon has been successfully explained by thermodynamic parameters [24, 25]. The change of the corrosion rate with the temperature was studied in in 1 M HCl. For this purpose, polarization curves were performed at different temperatures from 25 to 65°C in the absence and presence of different concentrations of R-DACH (Figs. 5 and 6). For 45 and 65°C, the electrochemical parameters were extracted and summarized in Tables 3 and 4. It is obvious that the values of J_{corr} increases by increasing the temperature in both solutions and the efficiency value decreases. Figures 5 and 6 show that raising the temperature has no significant effect on the corrosion potentials but leads to a higher corrosion rate. According to the Arrhenius equation, the apparent activation energy (E_a) of metal corrosion in both media (Blank

Table 2. Impedance spectroscopy data for steel corrosion in 1 M HCl solution with and without different concentration of inhibitor at 25°C

Concentration	R_s, Ω	R_{ct}, Ω	Q_{dl}, F	n
Blank	2.9	86	0.005	0.74
5×10^{-5}	3.1	131	3.00E-03	0.81
1×10^{-4}	2.8	430	1.00E-03	0.7
2×10^{-4}	9.1	582	8.00E-04	0.65
3×10^{-4}	13.3	618	8.00E-04	0.65
5×10^{-4}	13.6	621	5.00E-04	0.71
1×10^{-3}	14.5	679	7.00E-04	0.67
2×10^{-3}	14.7	751	8.00E-04	0.68

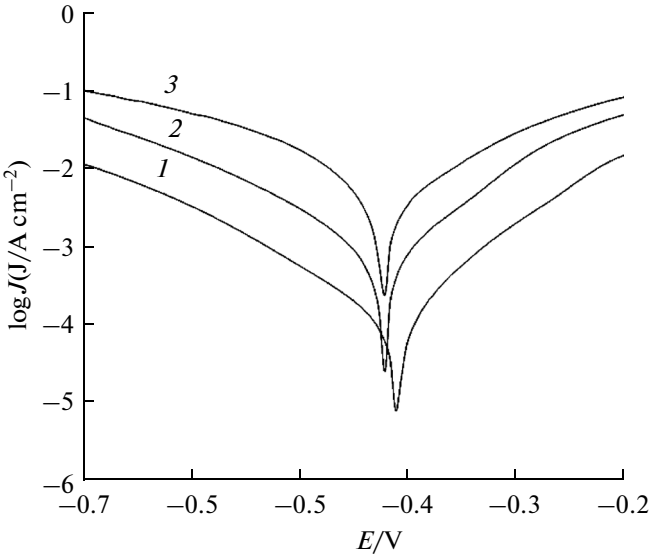

Fig. 5. Anodic and cathodic polarization curves of steel electrode in 1M HCl without inhibitor at different temperatures: (1) 25, (2) 45, (3) 65°C.

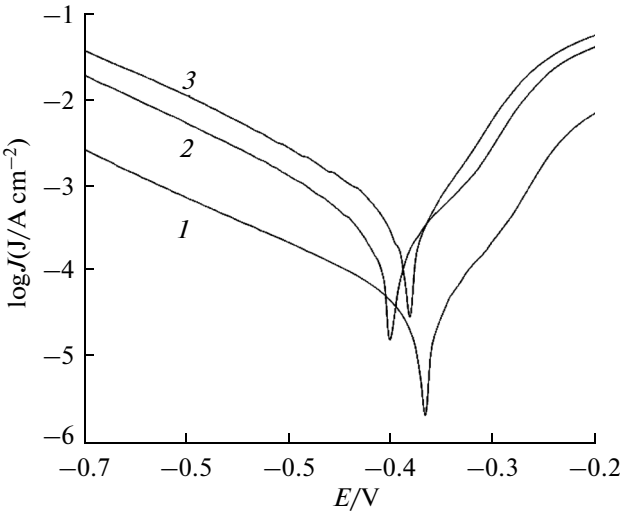

Fig. 6. Anodic and cathodic polarization curves of steel electrode in presence of 2×10^{-3} M of inhibitor at different temperatures: (1) 25, (2) 45, (3) 65°C.

and inhibited) can be calculated from the following equation [26]:

$$\ln J_{corr} = \ln A - \frac{E_a}{RT}, \quad (5)$$

where E_a represents the apparent activation energy, R is the gas constant, A is the pre-exponential factor, and T is the absolute temperature. Figure 7 shows the logarithm of J_{corr} against the reciprocal of temperature T^{-1} in the absence and presence of R-DACH. The activation energy E_a is calculated from the slope of the plots ($-E_a R^{-1}$). The calculated value of E_a in the absence of inhibitor is 58.5 kJ mol^{-1}, while in the presence of 2×10^{-3} M of inhibitor, it is 72.4 kJ mol^{-1}. It has been reported that higher E_a in presence of inhibitor for mild steel in comparison with blank solution typically shows physisorption [27]. Enthalpy and entropy of activation (ΔH_a, ΔS_a) are calculated from the transition state theory [27]:

$$J_{corr} = \left(\frac{RT}{Nh}\right)\exp\left(\frac{\Delta S_a}{R}\right)\exp\left(\frac{-\Delta H_a}{RT}\right), \quad (6)$$

where h is the Plank constant and N is the Avogadro's number. A plot of $\ln(J_{corr}\, T^{-1})$ versus T^{-1} gave straight lines as shown in Fig. 9 for mild steel dissolution in 1 M HCl in the absence and presence of different concentrations of R-DACH. Straight lines are obtained with a slope of $-\Delta H_a\ R^{-1}$ and an intercept of $\ln(RN^{-1}h^{-1}) + \Delta S_a R^{-1}$. The values of E_a, A, ΔH_a and ΔS_a are calculated and given in Table 5. The positive values of ΔH_a mean that the dissolution reaction is an endothermic process. Practically, E_a and ΔH_a are of the same order. Also, the entropy ΔS_a increases more positively with

Table 3. Potentiodynamic polarization parameters for the corrosion of steel in 1 M HCl solution in the absence and presence of different concentrations of inhibitor at 45°C

Concentration	β_c, mV	β_a, mV	J_{corr}, μA cm^{-2}	$-E$, mV	R_p, Ω cm^{-2}	θ	*IE*
Blank	181	108	969	408	30.31	–	–
5×10^{-5}	171	104	543	410	51.71	0.44	43.96
1×10^{-4}	167	102	380	399	72.36	0.61	60.78
2×10^{-4}	134	84.6	295	402.9	76.33	0.70	69.56
3×10^{-4}	122	77.9	233	395.2	88.60	0.76	75.95
5×10^{-4}	130	76.8	227	388.5	92.35	0.77	76.57
1×10^{-3}	116	76	192	392.5	103.84	0.80	80.19
2×10^{-3}	110	71	158	395.3	118.58	0.84	83.69

Table 4. Potentiodynamic polarization parameters for the corrosion of steel in 1 M HCl solution in the absence and presence of different concentrations of inhibitor at 65°C

Concentration	β_c, mV	β_a, mV	J_{corr}, μA cm^{-2}	$-E$, mV	R_p, Ω cm^{-2}	θ	*IE*
Blank	188	118	3990	403	7.89	–	–
5×10^{-5}	174	115	2423	419	12.41	0.39	39.27
1×10^{-4}	163	98	1654	421.7	16.07	0.59	58.55
2×10^{-4}	156	87	1110	407.5	21.85	0.72	72.18
3×10^{-4}	151	85.4	1060	408.6	22.35	0.73	73.43
5×10^{-4}	143	85	913	396	25.35	0.77	77.12
1×10^{-3}	122	88	832	397	26.68	0.79	79.15
2×10^{-3}	134	78	786	388	27.24	0.80	80.30

Table 5. Activation parameters of dissolution of steel in 1 M HCl solution in the absence and presence of inhibitor

Concentration, M	E_a, kJ mol^{-1}	A, A cm^{-2}	ΔH_a, kJ mol^{-1}	ΔS_a, J mol^{-1} K^{-1}	$E_a - \Delta H_a$, kJ mol−1
Blank	58.50	4.22E + 12	55.86	−8.63	2.64
5×10^{-5}	63.75	1.68269E + 13	61.11	−0.40	2.63
1×10^{-4}	62.33	6.90316E + 12	59.69	−7.81	2.63
2×10^{-4}	60.42	2.43995E + 12	57.78	−1.64	2.64
3×10^{-4}	63.32	6.24624E + 12	60.68	−8.64	2.63
5×10^{-4}	66.64	1.88399E + 13	64.01	0.53	2.63
1×10^{-3}	67.22	2.06348E + 13	64.59	1.30	2.64
2×10^{-3}	72.54	1.28635E + 14	69.91	16.51	2.63

the presence of the inhibitor. This reflects that the activated complex in the rate determining step represents dissociation rather than an association step, meaning that an increase in disordering takes place on going from reactants to the activated complex [6].

3.4. Adsorption Isotherm

Adsorption isotherms provide information about the interaction of the adsorbed molecules with the metal surface. The adsorption of organic compounds

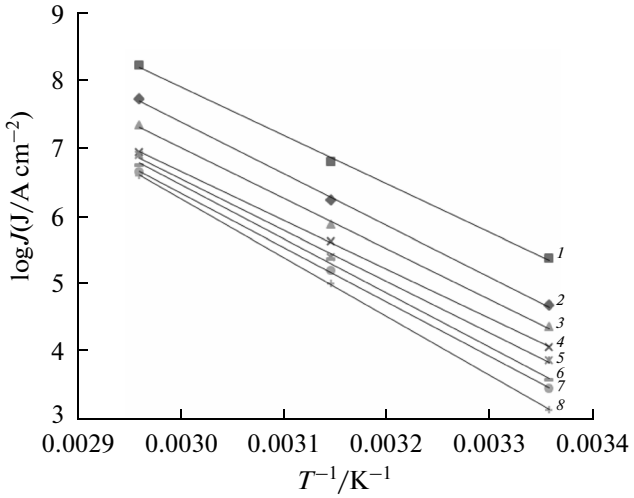

Fig. 7. Typical Arrhenius plots of lnJ_{corr} vs. T^{-1} for steel in 1 M HCl at different concentration of inhibitor : (■) Blank, (◆) 5×10^{-5}, (▲) 1×10^{-4}, (×) 2×10^{-4}, (*) 3×10^{-4}, (–) 5×10^{-4}, (●) 1×10^{-3}, (+) 2×10^{-3} M.

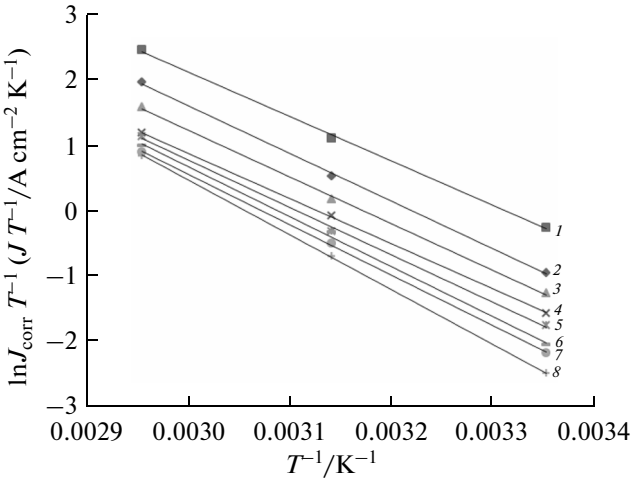

Fig. 8. Variation of lnJ_{corr} T^{-1} vs. T^{-1} for steel in 1 M HCl at different concentration of inhibitor: (■) Blank, (◆) 5×10^{-5}, (▲) 1×10^{-4}, (×) 2×10^{-4}, (*) 3×10^{-4}, (–) 5×10^{-4}, (●) 1×10^{-3}, (+) 2×10^{-3} M.

can be expressed by two main types of interactions: physical adsorption and chemical adsorption. There are some factors that influence the adsorption processes including the nature and charge of metal, the chemical of inhibitor, and the type of electrolyte [28].

The adsorption of an organic adsorbate at metal/solution interface can be presented as a substitution adsorption process between the organic molecules in aqueous solution, $Org_{(sol)}$, and the water molecules on metallic surface, $H_2O_{(ads)}$:

$$Org_{(sol)} + xH_2O_{(ads)} \longleftrightarrow Org_{(ads)} + xH_2O_{(sol)}, \quad (7)$$

where $Org_{(sol)}$ and $Org_{(ads)}$ are the organic species dissolved in the aqueous solution and adsorbed onto the metallic surface, respectively, $H_2O_{(ads)}$ is the water molecule adsorbed on the metallic surface, $H_2O_{(sol)}$ is water molecule in solution, and x is size ratio and represents the number of molecules of water replaced by inhibitor molecule.

Different adsorption isotherms, Langmuir, Temkin, Freundlich, Frumkin, Modified, Langmuir, Henry, Viral, Damaskin, Volmer, and Flory-Huggins, [29, 30] were tested for their fit to the experimental data. The linear regression coefficient values (R^2) were determined from the plotted curves. According to these results it was found that the experimental data obtained from polarization readings could be fitted by Langmuir's adsorption isotherm. According to this isotherm, the surface coverage is related to inhibitor concentration by [30, 31]:

$$\frac{\theta}{1-\theta} = K_{ads}C, \quad (8)$$

$$\frac{C}{\theta} = \frac{1}{K_{ads}} + C, \quad (9)$$

where K_{ads} is the equilibrium constant of the inhibitor adsorption process, C is the inhibitor concentration and θ is the surface coverage that was calculated by Eq. (1).

A fitted straight line is obtained for the plot of $C\theta^{-1}$ versus C with slopes close to 1 as seen in Fig. 9. The strong correlation ($R^2 > 0.99$) suggests that the adsorption of R-DACH on the mild steel surface obeys Langmuir's adsorption isotherm. This isotherm assumes that the adsorbed molecules occupy only one site and there are no interactions with other adsorbed species [30]. The K_{ads} values can be calculated from the intercept lines on the $C\theta^{-1}$ -axis. This is related to the standard free energy of adsorption (ΔG_{ads}) with the following equation [32]:

$$\Delta G_{ads} = -RT\ln(55.5K_{ads}), \quad (10)$$

where R is the gas constant and T is the absolute temperature. The constant value of 55.5 is the concentration of water in solution in Molar. The enthalpy and entropy of adsorption (ΔH_{ads} and ΔS_{ads}) can be calculated using the following equations [23]:

$$\Delta G_{ads} = \Delta H_{ads} - T\Delta S_{ads}, \quad (11)$$

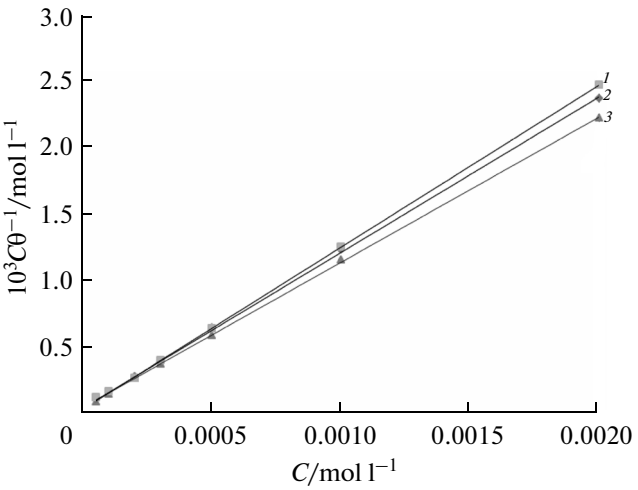

Fig. 9. Langmuir adsorption isotherm $C\theta^{-1}$ vs. C of inhibitor in 1 M HCl at different temperatures: (■ 25°C, ◆ 45°C, ▲ 65°C).

$$\ln K_{ads} = -\frac{\Delta H_{ads}}{RT} + \frac{\Delta S_{ads}}{R} - \ln(55.5). \quad (12)$$

The negative values of ΔG_{ads} suggest that the adsorption of R-DACH on the steel surface is spontaneous. Generally, the values of $-\Delta G_{ads}$ around or less than 20 kJ mol^{-1} are associated with the electrostatic interaction between charged molecules and the charged metal surface (physisorption); while those around or higher than 40 kJ mol^{-1} mean charge sharing or transfer from the inhibitor molecules to the metal surface to form a coordinate type of metal bond (chemisorption). The values of K_{ads} and ΔG_{ads} are listed in Table 6. The ΔG_{ads} values are around −36 kJ mol^{-1}, which means that the absorption of inhibitor on the steel surface belongs to both physisorption and chemisorption, and the adsorptive film has an electrostatic character [20]. Figure 10 represents the plots of $\ln K_{ads}$ versus T^{-1} for adsorption R-DACH. The obtained lines can provide valuable information about the mechanism of corrosion inhibition. An endothermic adsorption process $\Delta H_{ads} > 0$ is attributed unequivocally to chemisorption, and an exothermic adsorption

Table 6. Thermodynamic and equilibrium adsorption parameters for adsorption of inhibitor on steel surface in 1 M HCl solution

T, K	K_{ads}, M^{-1}	ΔG_{ads}, KJ mol^{-1}
298	−34.37	19083.97
318	−36.55	18214.94
338	−38.71	17361.11

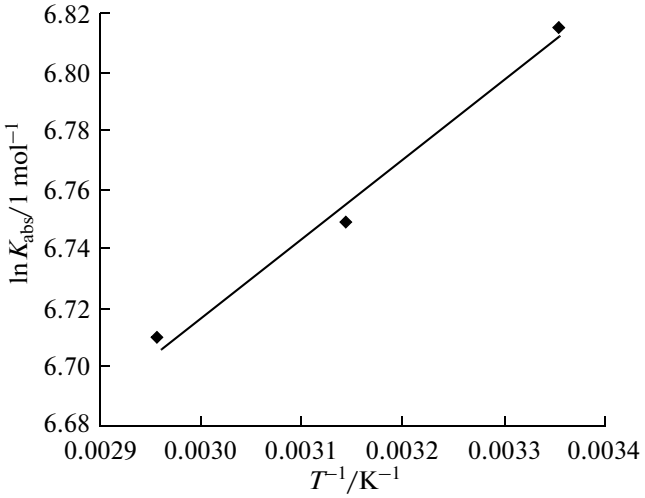

Fig. 10. $\ln K_{ads}$ vs. T^{-1} for inhibitor adsorption on steel surface.

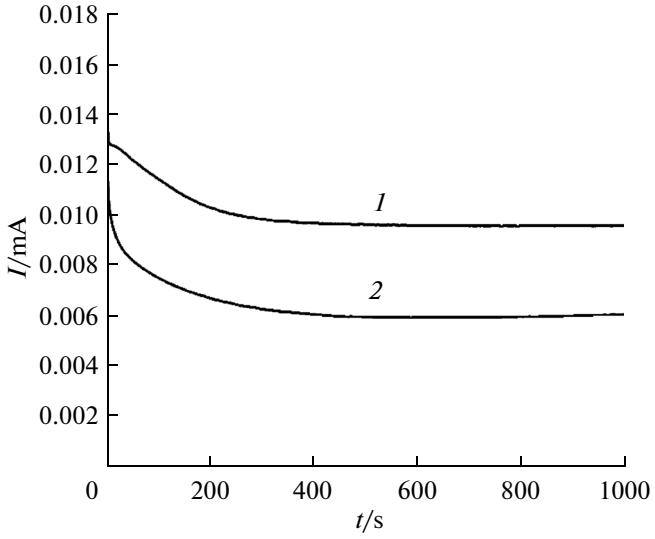

Fig. 11. Current transients of steel electrode at −0.3 V vs. SCE: (1) Blank, (2) 2×10^{-3} M of inhibitor.

process $\Delta H_{ads} < 0$ may involve either physisorption or chemisorption or a mixture of both processes [33]. The calculated values of ΔH_{ads} and ΔS_{ads} are −1.97 kJ and 108.71 J mol^{-1} K^{-1}, respectively. The calculated ΔG_{ads} and ΔH_{ads} values for inhibitor show that the adsorption mechanism is not completely physical or chemical, and a combination of physisorption and chemisorption exists between the inhibitor and metal surface. The positive sign of ΔS_{ads} arises from the substitution process, which can be attributed to the increase in the solvent entropy and more positive water desorption entropy. It is also interpreted with an increase of disorders due to the more water molecules which can be desorbed from the metal surface by one inhibitor molecule [21]

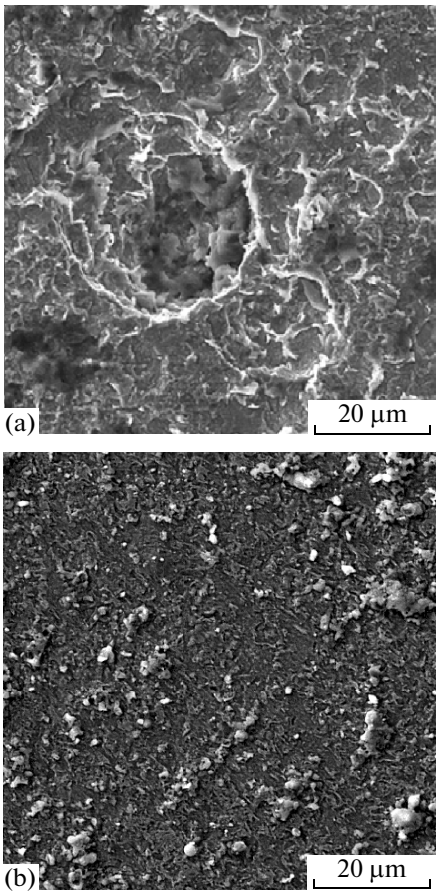

Fig. 12. Scanning electron microscopyimages of steel exposed to 1 M HCl solution (a) in the absence of inhibitor (b) in the presence of 2×10^{-3} M of inhibitors.

3.6. Chronoamperometry

In order to gain more insight about the effect of R-DACH on the electrochemical behavior of steel in 1 M HCl solution, potentiostatic current-time transients were recorded. Figure 11 shows the current transients of steel electrode at −0.3 V (vs. SCE) applied anodic potential. Initially the current decreases monotonically with time, and the decrease in the current density is due to the formation of corrosion products layer on the anode surface. However, in later time, the current reaches to a steady state value due to the steel dissolution depending on applied potential (Fig. 11). In presence of inhibitor, the dissolution current decreased and electrode inhibited from corrosion due to inhibitor adsorption.

3.7. Scanning Electron Microscopy

In order to evaluate the conditions of the steel surfaces in contact with hydrochloric acid solution, surface analysis was carried out. Surface was observed before and after 12 h of immersion in 1 M HCl in the absence and presence of R-DACH at 25°C. Scanning

electron microscopy (SEM) studies of the surface in the absence and presence of inhibitor are presented in Fig. 12. The SEM reveals the presence of corrosion attack and some pits on the surface in the absence of inhibitor while such damages are diminished in the presence of inhibitor.

4. CONCLUSION

1. The synthetic Schiff base R-DACH acts as an inhibitor for mild steel corrosion in 1 M HCl solution, especially in high concentration.

2. Inhibition efficiency of this compound increases with increasing their concentrations due to the formation of a film on the steel. The inhibitor decreased both anodic and cathodic Tafel current, which showed the mixed mode of action of the inhibitor molecules.

3. The inhibition of mild steel in 1 M HCl solution at different temperatures was found to obey the Langmuir adsorption isotherm.

4. The negative values of ΔG indicate the spontaneous adsorption of the inhibitor on the surface of mild steel.

5. Surface studies show that the surface of sample in solution with inhibitor molecules looks more flat and more uniform with lower roughness than that in the uninhibited solution.

REFERENCES

1. Kayadibi, F., Sagdinc, S.G., and Kara, Y.S., *Prot. Met. Phys. Chem. Surf.*, 2015, vol. 51, p. 143.
2. Sobhi, M., *Prot. Met. Phys. Chem. Surf.*, 2014, vol. 50, p. 825.
3. Zor, S., *Prot. Met. Phys. Chem. Surf.*, 2014, vol. 50, p. 530.
4. Ghasemi, O., Danaee, I., Rashed, G.R., et al., *J. Cent. South Univ. Technol.* (Engl. Ed.), 2013, vol. 20, p. 301.
5. Shalabi, K., Fouda, A.S., Elewady, G.Y., and El-Askalany, A., *Prot. Met. Phys. Chem. Surf.*, 2014, vol. 50, p. 420.
6. Jafari, H., Danaee, I., Eskandari, H., and Rashvandavei, M., *Ind. Eng. Chem. Res.*, 2013, vol. 52, p. 6617.
7. Sagdinc, S.G. and Kara, Y.S., *Prot. Met. Phys. Chem. Surf.*, 2014, vol. 50, p. 111.
8. Avdeev, Y.G., Luchkin, A.Y., and Kuznetsov, Y.I., *Prot. Met. Phys. Chem. Surf.*, 2013, vol. 49, p. 865.
9. Shpan'ko, S. P., Grigor'ev, V.P., Anisimova, V.A., et al., *Prot. Met. Phys. Chem. Surf.*, 2013, vol. 49, p. 859.
10. Gholami, M., Danaee, I., Maddahy, M.H., and Rashvandavei, M., *Ind. Eng. Chem. Res.*, 2013, vol. 52, p. 14875.
11. Abdallah, M., Asghar, B.H., Zaafarany, I., and Sobhi, M., *Prot. Met. Phys. Chem. Surf.*, 2013, vol. 49, p. 485.
12. Baghaei Ravari, F. and Dadgareenezhad, A., *Prot. Met. Phys. Chem. Surf.*, 2015, vol. 51, p. 138.
13. Danaee, I., Ghasemi, O., Rashed, G.R., et al., *J. Mol. Struct.,* 2013, vol. 1035, p. 247.
14. Fouda, A.S., Abdallah, M., and Medhat, M., *Prot. Met. Phys. Chem. Surf.,* 2012, vol. 48, p. 477.
15. Macdonald, J.R., *Solid State Ionics*, 1984, vol. 13, p. 147.
16. Danaee, I., *J. Electroanal. Chem.*, 2011, vol. 662, p. 415.
17. Negm, N.A., Elkholy, Y.M., Zahran, M.K., and Tawfik, S.M., *Corros. Sci.*, 2010, vol. 52, p. 3523.
18. Hegazy, M.A., *Corros. Sci.*, 2009, vol. 51, p. 2610.
19. Keles, H., *Mater. Chem. Phys.*, 2011, vol. 130, p. 1317.
20. Emregul, K.C. and Atakol, O., *Mater. Chem. Phys.*, 2003, vol. 82, p. 188.
21. Hoseinzadeh, A.R., Danaee, I., and Maddahy, Y.M.H., *Z. Phys. Chem.*, 2013, vol. 227, p. 403.
22. Danaee, I., Niknejad Khomami, M., and Attar, A.A., *Mater. Chem. Phys.*, 2012, vol. 135, p. 658.
23. Hoseinzadeh, A.R., Danaee, I., and Maddahy, M.H., *J. Mater. Sci. Technol.*, 2013, vol. 29, p. 884.
24. Badr, G.E., *Corros. Sci.*, 2009, vol. 51, p. 2529.
25. Hegazy, M.A., Ahmed, H.M., and El-Tabei, A.S., *Corros. Sci.*, 2011, vol. 53, p. 671.
26. Aljourani, J., Raeissi, K., and Golozar, M.A., *Corros. Sci.*, 2009, vol. 51, p. 1836.
27. Herrag, L., Chetouani, A., Elkadiri, S., et al., *Port. Ectrochim. Acta*, 2008, vol. 26, p. 211.
28. Oguzie, E.E., Unaegbu, C., Ogukwe, C.N., et al., *Mater. Chem. Phys.*, 2004, vol. 84, p. 363.
29. Mu, G., Li, X., Qu, Q., and Zhou, J., *Corros. Sci.*, 2006, vol. 48, p. 445.
30. Bayol, E., Gurtenb, T., Gurtena, A.A., and Erbil, M., *Mater. Chem. Phys.*, 2008, vol. 112, p. 624.
31. Keles, H., Keles, M., Dehri, I., and Serindag, O., *Mater. Chem. Phys.,* 2008, vol. 112, p. 173.
32. Dogru Mert, B., Erman Mert, M., Kardas, G., and Yazici, B., *Corros. Sci.*, 2011, vol. 53, p. 4265.
33. Li, X.H., Deng, S.D., Fu, H., and Mu, G.N., *Corros. Sci.*, 2009, vol. 51, p. 2639.